

Intermediates in the Reaction of NO_x Reduction with Propane over Cu/ZSM-5 Catalysts (by ESR, TPD, and IR-Spectroscopy *in Situ*)

V. A. Matyshak, A. N. Il'ichev, A. A. Ukharsky, and V. N. Korchak

Heterogeneous Catalysis Laboratory, N. N. Semenov Institute of Chemical Physics, Russian Academy of Science, ul. Kossygin 4, Moscow, 117334, Russia

Received March 19, 1996; revised May 27, 1997; accepted June 4, 1997

On the base of ESR, TPD, and IR-spectroscopy *in situ* data, the $\text{Cu}^{2+}\text{-O-N=O}$ complex is found to be formed on the surface of Cu-containing zeolites in the reduction of NO by propane under oxygen excess. The spectrokinetic method was used to measure the rate of further conversion of this complex to the reaction products. It appeared to be equal to the reaction rate. Coincidence of these two rates implies that the $\text{Cu}^{2+}\text{-O-N=O}$ complex is a true intermediate in this reaction and takes part in the rate-determining stage. $\text{Cu}_{\text{isol}}^{2+}$ ions in the samples studied are the centers where one of the first stages of the reaction (NO activation) proceeds. The next stages occur, possibly, over other surface states of the copper. From this point of view, the $\text{Cu}_{\text{isol}}^{2+}$ ions is a necessary part of the complex active center of the reaction. © 1997 Academic Press

INTRODUCTION

The recent discovery of using hydrocarbon as a selective reducing agent for the transformation of NO to N_2 over metal-exchanged zeolites (1, 2) has stimulated research activity in this area considerably. However, only limited data are available on the nature and properties of the surface complexes formed during adsorption of reagents and, particularly, on their role in the reaction. Some published data (3–23) are presented in Table 1. Their reliability (low, middle, and high, marked off by L, M, and H, correspondingly) depends essentially upon the experimental conditions: L—data obtained before or after the reaction; M—*in situ* data; and H—investigations where kinetics of the transformation of surface complexes has been studied and correlated with the reaction kinetics. Unfortunately, most of the studies were performed under conditions that were not close to the conditions of the catalytic reaction. That is why there is no unified point of view on the mechanism of the reduction of NO_x over Cu-containing zeolites in the presence of an excess of oxygen.

Several reaction schemes are considered as being probable:

Authors to whom correspondence should be addressed: V. A. Matyshak/N. N. Semenov. Fax: 007 095 938 21 56.

1. NO is oxidized to NO_2 or nitrite/nitrate complexes (NO_x), which then interact with hydrocarbons (24–33).
2. Hydrocarbons are converted to some intermediates which then interact with NO_x (34–37).
3. A redox mechanism of the catalyst surface oxidation by NO_x and reduction by hydrocarbons operates (38, 39).

Although the activity of the exchanged CuZSM-5 has been well reproducible, its origin is still the subject of controversy. The mechanism of SCR of NO involving monovalent copper (Cu(I)) as an active site is favored by Iwamoto (40) and Cho (41). In papers (29, 42, 43) good evidence for the importance of bivalent copper (Cu(II)) in the SCR of NO in lean-burn exhaust gas conditions is presented.

In the over-exchanged zeolite the observations by XPS/XAES, XANES methods (5, 44, 45) shows that copper is present as isolated Cu^{2+} and Cu^+ ions inside the zeolite structure and as CuO- and Cu_2O -like aggregates are on the outer surface of the zeolite. The size of these aggregates were not discussed in the cited papers.

The results of (45) indicate that Cu(II) species (CuO and $\text{Cu}_{\text{isol}}^{2+}$) are the active centers for the SCR of NO. Evidence for the importance for SCR of NO to be a ready conversion between Cu(I) and Cu(II) and possible between clusters and ions is presented in (5, 44).

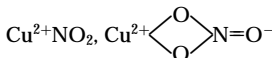
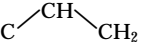
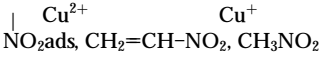
Copper aggregates have been postulated as possible active sites by Petunchi (16).

The preparation procedure (excess ion exchange) was believed to promote also the formation of oxocation $[\text{Cu-O-Cu}]^{2+}$ or pairs $[\text{Cu(II)-O-Cu(II)}]$ (27, 46–49). These copper species are considered as active sites for NO or N_2O decomposition (50, 51).

In our understanding of these catalysts several important questions remain open. Thus the reduction of Cu(II) ions in ZSM-5 to Cu(I) appears to be facile (5, 27, 44, 49, 52). On the other hand, some reports suggest a considerable stability of Cu(II) towards reduction in ZSM-5 (53–55), casting doubt on the relevance of redox mechanisms in the SCR of NO_x .

For understanding the mechanism of SCR of NO we need more detailed information on the processes going on over

TABLE 1
Intermediates in NO Decomposition and Reduction
by Hydrocarbons

Reaction, catalyst	Intermediates	Degree of Refer-	reliability	ences
Decomposition of NO on Cu-ZSM5	O _{ads}	M	3	
	Cu ⁺ NO, Cu(NO) ₂ , Cu(NO ₂) ⁻	M	4	
	(Cu-O-Cu) ²⁺ , CuOH ⁺	L	5, 6	
	CuNO, Cu(NO) ₂	M	7	
	Cu ⁺ NO ^{δ-} , Cu ⁺ (NO) ₂ ^{δ-} , Cu ²⁺ NO ^{δ+}	M	8	
C ₃ H ₆ + NO + O ₂ on Cu-ZSM5	Cu ⁺ (NO) ₂ , Cu ²⁺ (O)(N ₂ O)	M	9	
	Cu ²⁺ (O ⁻)(NO), Cu ²⁺ (NO)(NO ₂)	H	10	
	Cu ²⁺ -N=N, Cu ²⁺ NO, Cu ⁺ NO			
	Cu ⁺ (NO) ₂ , Cu ²⁺ -O-N=O,			
				
	Cu ⁺ NO, Cu ²⁺ (NO)(NO ₂),	M	9	
	CH ₂ =CH-CH ₃ , H ₂ C- 	M	11	
				
	NO _{2ads} , CH ₂ =CH-NO ₂ , CH ₃ NO ₂			
	HCN, CH ₃ CN			
CN, NCO	M	12		
Cu ⁺ (NO) ₂ , Cu ⁺ Oads	L	13		
NCO, C _m H _n , C _x H _y O, NOads	M	14		
C ₃ H ₈ + NO + O ₂ on Cu-ZSM5	NO _{2ads} , C _x H _y O	L	15	
<i>i</i> -C ₄ H ₈ + NO + O ₂ on Cu-ZSM-5	C _x , NOads	L	16	
C ₃ H ₆ + NO + O ₂ on Ce-ZSM-5	NO ₂ ⁻ , NO ₃ ⁻ , CH ₃ NO ₂ , NCO	H	17, 18	
CH ₄ + NO + O ₂ on Ga-ZSM-5	CH _{3ads}	L	19-21	
C ₃ H ₆ + NO + O ₂ on Rh/Al ₂ O ₃	C ₃ H _{5ads} , HNO _x	L	22	
C ₃ H ₈ + NO + O ₂ on ZrO ₂ and mixed oxides	R-NO _x , NO _x , NCO, NO ₂ , NO ₃ ⁻	M	23	

the surface of the catalyst. Here we make an attempt to reveal the nature of the intermediates and the role of Cu ions in various valence and coordination states in the reaction of NO_x reduction by propane over Cu/ZSM-5 zeolites.

EXPERIMENTAL

Samples containing 0.15, 0.70, 1.3, 1.7, and 2.8 wt% Cu were prepared on the base of HZSM-5 zeolite (in the following this will be referred to as CuZ(1)). The sample containing 2.86 wt% Cu was prepared on the base of NaHZSM-5 zeolite (in the following this will be referred to as CuZ(2)). The sodium form of ZSM-5 zeolite (Si/Al = 40, crystallinity 90%, no iron impurities were detected by ESR)

was used as a starting sample for all the samples. The ratio of Na/Al was about 0.4 in CuZ(2) and less than 0.02 in CuZ(1).

The samples were prepared by ion exchange from an aqueous solution of copper sulfate (56) during 6 h followed by drying at 373 K and calcination at 823 K. No sulfate ions in the samples were detected by IR-spectroscopy, as well as no appreciable influence of SO₄²⁻ ions on the configuration of isolated Cu²⁺ ions (Cu_{isol}²⁺) was found by ESR.

Measurements were performed both on the oxidized (823 K, O₂, 1 h) and reduced (823 K, H₂, 1 h) catalysts.

The samples were tested in the reduction of NO with C₃H₈ (reaction mixture: 0.24% NO + 0.24% C₃H₈ + 5% O₂). Gas hourly space velocity (GHSV) was 20000 h⁻¹. Inlet and outlet gases were analyzed by a Beckman gas analyzer (CO, NO₂, NO, C₃H₈) and by gas chromatography (O₂, CO₂, N₂O).

Copper in Cu-containing zeolites is known to be in both isolated (Cu²⁺, Cu⁺ ions) and associated (CuO- or Cu₂O-like aggregate) states.

The concentration and configuration of isolated Cu²⁺ ions (Cu_{isol}²⁺) were determined by ESR. ESR spectra were recorded (by ESR-B spectrometer) at room temperature under vacuum or flow conditions after treatment of the sample by gas pulses (102–103 Pa, 5 min) at various temperatures (300–943 K). CuSO₄ · 5H₂O was used as a standard. Spin concentration was determined with accuracy about 10%.

The concentration of Cu⁺ ions was derived from TPD spectra of CO, for it is known (1, 57) that above room temperature CO molecules are bound strongly only with Cu⁺ ions. Determination of the Cu⁺ concentration was accurate to 20%.

The amount of copper in the CuO and Cu₂O aggregates (Cu_a) for oxidized samples was found as a difference between the overall copper content in the sample and the sum amount of the Cu_{isol}²⁺ and Cu⁺ ions.

Interaction of the reactants with the catalyst surface was studied by TPD under vacuum conditions (heating rate 12 K/min) and IR-spectroscopy *in situ*. Properties of the surface compounds formed during the process were studied by the spectrokinetic method (58, 59). This method implies the simultaneous measurements of the reaction rate and the rate of conversion of surface species.

The setup for spectroscopic and spectrokinetic measurements included a UR-20 spectrometer modified so as to provide the possibility of high-temperature measurements, a heated flow cell (volume 1 cm³) (59) which served simultaneously as a catalytic reactor, a unit for gas purification, and a system for analysis of products and reagents. The overall flow rate was 150 ml/min. Experiments were performed with pellets of the samples; the weight of the pellet was 10–15 mg/cm²; the surface area was ~2 cm². Details of the experimental procedure are described in (59).

TABLE 2
NO Conversion on Cu/ZSM-5 Zeolites

Catalysts	Cu concentration [Cu]%w	NO conversion (%)		
		673 K	773 K	873 K
CuZ(1)	0, 15	15	22	28
	0, 7	25	40	30
	1, 3	40	47	35
	1, 7	43	60	55
	2, 8	50	65	63
CuZ(2)	2, 86	0	30	35

RESULTS

I. Catalytic Activity and the State of the Copper in the Samples

Data on the catalytic activity in the reduction of NO by propane are summarized in Table 2. Nitrogen is the main reaction product. At low temperature trace amounts of N₂O were detected. The activity of the zeolite without Cu at 673–873 K is close to zero.

According to ESR-data, concentration of Cu_{isol}²⁺ ions in the active samples after the reaction (reaction time = 2 h, *T* = 773 K) is close to that determined after the treatment of the sample in oxygen at 873 K.

Typical ESR spectra of Cu-containing zeolites are shown in Fig. 1. The spectra parameters for all the samples are presented in Table 3. ESR spectra show that Cu_{isol}²⁺ ions in all the samples studied (oxidized and reduced) are arranged in square pyramidal and plane square configurations (53, 54). Additional splitting of the *g*_{||}⁽¹⁾ component implies that there could be two slightly different square pyramidal configurations of Cu_{isol}²⁺ ions (Fig. 1, spectrum 1).

It is worth noting that the ratio of intensities of Cu_{isol}²⁺ signals in different configurations for reduced and oxidized samples is essentially constant and close to one.

TABLE 3

Parameters of the ESR Spectra of the Catalysts under Study

Sample	Pretreatment conditions	<i>g</i>	<i>A</i>	<i>g</i> _⊥	<i>A</i> _⊥	Coordination
CuZ(1)	TV ^a	2.33	168	2.07	16	Pyramid
	520–930 K	2.32	168	—	—	Pyramid
		2.29	180	2.03	25	Square
		Reduction	2.33	165	2.065	15
	H ₂ , 823 K	2.316	165	—	—	Pyramid
		2.285	185	2.04	27	Square
Oxidation	O ₂ , 823 K	2.33	167	—	—	Pyramid
	2.29	185	—	—	Square	
CuZ(2)	TV ^a	2.31	163	2.06	16	Pyramid

^a Thermovacuum treatment.

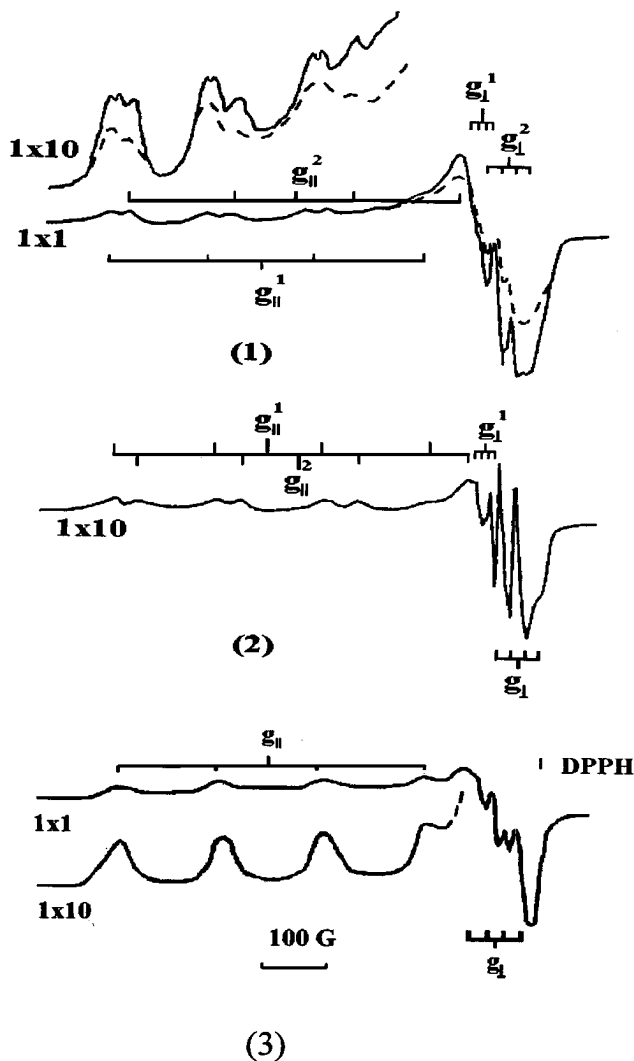


FIG. 1. ESR spectra of 1.3% CuZ(1) in (1) oxidized and (2) reduced states. Spectrum (3) is related to 2.86% CuZ(2) sample oxidized.

For oxidized samples, the intensity of the Cu_{isol}²⁺ signal is high (Fig. 1, spectrum 1), but hyperfine (hf) lines in the *g*_⊥ region are poorly resolved. This makes it impossible to determine the splitting constant *A*_{||}. On the contrary, for reduced (at 873 K) samples, the intensity of the Cu_{isol}²⁺ signal is lower, but the spectrum exhibits better resolution (spectrum 2).

Noteworthy is the high thermal stability of the Cu_{isol}²⁺ state. Treatment of the oxidized and reduced samples in a vacuum within the temperature range from 400 to 950 K does not change the ESR signal of Cu_{isol}²⁺ ions.

It should be pointed out that Cu_{isol}²⁺ ions in the plane square configuration were not detected in the CuZ(2) sample (Fig. 1, spectrum 3). This result is in agreement with the data published in (54).

Concentration of copper in various oxidation states (Cu_{isol}²⁺, Cu⁺, Cu_a) versus total copper content in the samples

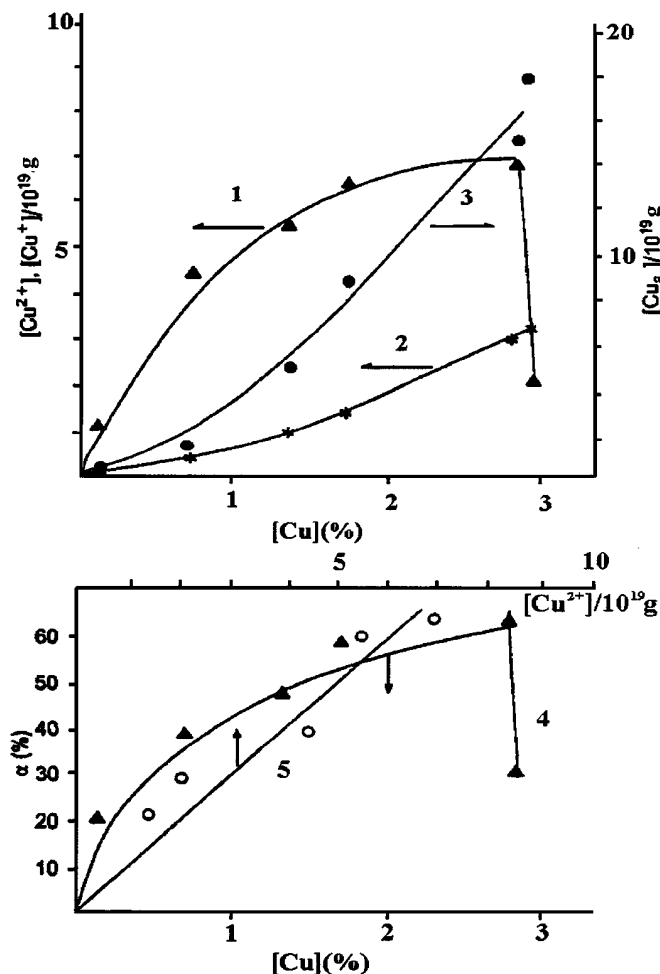


FIG. 2. Dependence of the concentrations of (1) Cu^{2+} , (2) Cu^+ , (3) Cu_a , and (4) NO conversion (α %) at $T=773$ K versus copper concentration in oxidized samples; (5) presents the relationship between NO conversion (α %) and $\text{Cu}_{\text{isol}}^{2+}$ concentration.

is displayed in Fig. 2. As is seen, Cu_a and Cu^+ ions always exist in the oxidized samples, and their concentration increases with the total copper content. Concentration of $\text{Cu}_{\text{isol}}^{2+}$ ions also grows with the total copper content for the CuZ(1). However, for the CuZ(2) sample with the same total copper content (2.86%) it is essentially lower (Fig. 2, curve 1). In the samples with a low Cu content all copper ions are essentially isolated, whereas in samples with high copper content, they at most form aggregates (Fig. 2, curve 3). Curve 4 on Fig. 2 displays the dependence of the conversion of NO (α %) at 773 K on the copper content in the samples. It correlates well with curve 1 (concentration of $\text{Cu}_{\text{isol}}^{2+}$ ions).

II. Adsorption of Reagents

1. NO Adsorption

We failed to observe any absorption bands of nitrosil complexes in transmission and diffuse-reflectance IR spec-

tra (concentration of NO was varied from 0.1 to 20% in the temperature range from 300 to 783 K, oxidized and reduced samples were studied). Only two weak absorption bands (at 1570 and 1430 cm^{-1}) attributed to nitrate surface complexes were observed.

The adsorption of NO at 293 K and 0.8 kPa results in a decrease of hf lines intensity without any change of their parameters (this spectrum is shown by the dashed line in Fig. 1). This phenomenon, observed by other investigators also (55, 60), is likely to be due to the interaction of paramagnetic NO molecules with $\text{Cu}_{\text{isol}}^{2+}$ ions followed by the formation of some weak complexes. When NO gas is pumped out from the reactor, these complexes are destroyed quickly and the ESR-spectra of the samples are restored to their original form. We failed to detect any ESR spectra of Cu^+ -NO complexes at 293 K and 0.1–800 Pa (the concentration of Cu^+ ions was varied from $0.1 \cdot 10^{19}$ to $9 \cdot 10^{19} \text{ g}^{-1}$). These complexes were observed by Anpo *et al.* at 77–273 K (61). It is worth noting that heating the reduced sample in the presence of NO from 470 to 853 K and in 0.01–0.8 kPa range did not cause any increase in the intensity of the ESR-spectra of $\text{Cu}_{\text{isol}}^{2+}$ ions. In other words, reduced copper ions are not oxidized in the presence of NO.

TPD spectra of the samples after adsorption of NO (Fig. 3, spectrum 4) reveal only one peak with the maximum at $T_{\text{max}}=370$ K. As follows from the analysis of the desorption products, this peak is mainly due to NO desorbed from zeolite itself.

All the data obtained suggest that at 300 K NO is adsorbed predominantly on the zeolite. Weakly bound NO molecules are desorbed at 360–380 K.

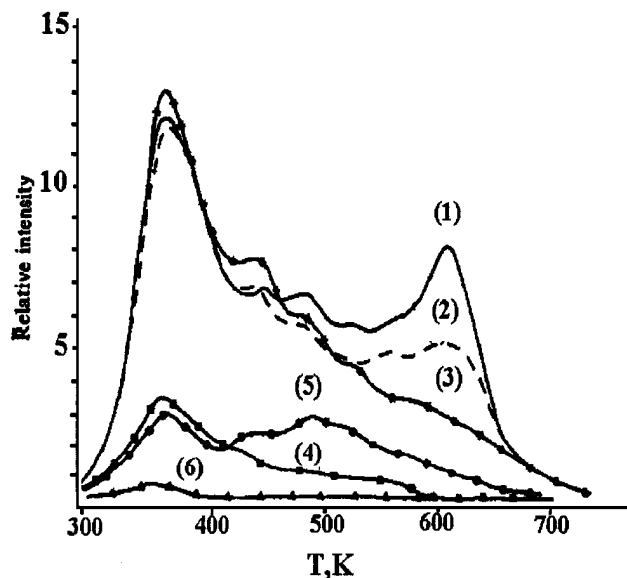


FIG. 3. TPD spectra after NO + O_2 adsorption on the reduced (1), oxidized, (2) catalyst and zeolite without copper, (3) $P=0.8$ kPa, $T=293$ K, the adsorption time 50 min. Spectra after adsorption of NO (4); NO, then O_2 (5); and O_2 (6) for the reduced catalyst.

2. Adsorption of Oxygen

According to ESR-data, during the adsorption of O₂ at room temperature, as well as during the adsorption of NO, weakly bound complexes are formed on the surface of the samples. Their formation is followed by a decrease of the hf lines intensity.

TPD spectrum after the adsorption of oxygen (Fig. 3, spectrum 6) reveals a low-intensity peak with $T_{\max} = 350$ K. When the sample reduced is heated in the presence of oxygen (from 470 to 853 K), the intensity of the Cu_{isol}²⁺ signal increases.

3. Adsorption of the NO + O₂ Mixture

At the adsorption of the NO + O₂ mixture (0.24% NO and 5% O₂) the absorption band at 1630 cm⁻¹ is observed in the IR-spectra. Its intensity (D) increases when oxygen or NO content rises. In the presence of the mixture the band at 1630 cm⁻¹ is detected in the IR-spectra after heating the sample up to 600 K. It is assigned to the vibrations in the Cu²⁺-O-N=O complex (10).

ESR-spectra of the samples changes significantly during the adsorption of a 1 : 1 NO + O₂ gas mixture ($P = 0, 8$ kPa, $T = 293$ K) (compare spectra 1 for the oxidized sample and spectra 2 for the reduced one, presented in Figs. 1 and 4).

Figure 5 shows typical ESR-spectra (in the g_{\perp} range) of the prereduced catalyst during the adsorption of NO + O₂ mixture at different moments of time. As is seen, during

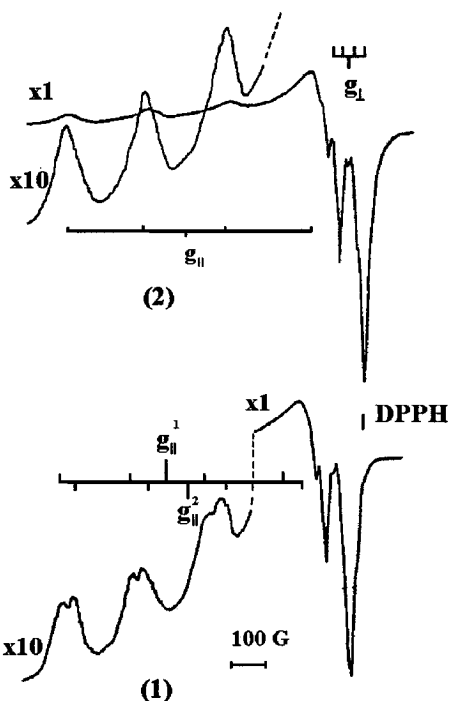


FIG. 4. ESR spectra of the oxidized (1) and reduced (2) catalyst after NO + O₂ adsorption ($P = 0.8$ kPa, $T = 293$ K).

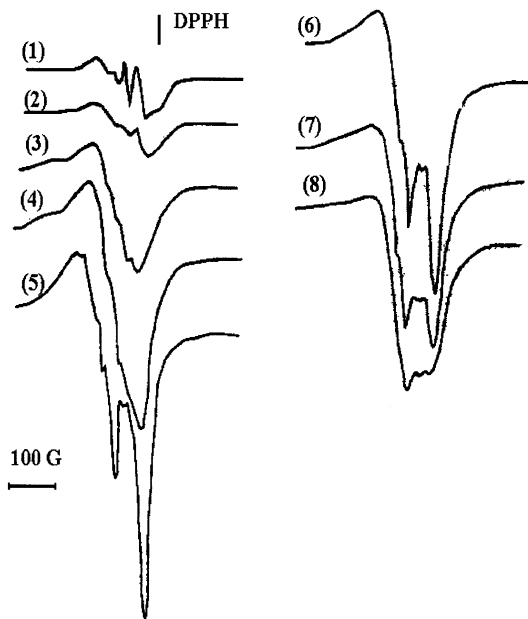


FIG. 5. ESR spectra of the catalyst during adsorption of NO + O₂ mixture ($P = 0.8$ kPa, $T = 293$ K) registered at $t = 0$ min (1), 2 (2), 13 (3), 24 (4), 30 (5), 36 (6), 39 (7), 50 (8).

the first 25 min of adsorption the intensity of the signal increases. It means that the concentration of Cu_{isol}²⁺ ions in the sample increases. After next 10 min a new spectrum (curve 5) appears. Then the intensity of the signal decreases and the hf lines disappear (curves 6–8). These changes of the spectrum seem to be due to a weak interaction between Cu_{isol}²⁺ ions and paramagnetic NO, NO₂, and O₂ molecules, since pumping out the gas results in restoration of the previous spectrum (curve 5).

Note, that the ESR-spectra of the preoxidized sample are not essentially changed during the first 20 min of the NO + O₂ adsorption (the stage of oxidation is absent). Then the spectrum changes similarly to that one which is observed in the case of the prereduced sample during the adsorption for more than 20 min. Recently similar spectra have been obtained for Cu/ZSM-5 samples even at 600 K in flow conditions (7).

Comparison of spectra presented in Figs. 1 and 4 (curves 1, 2, i.e., before and after NO + O₂ adsorption) shows that the configuration of Cu_{isol}²⁺ ions during NO + O₂ adsorption changes. The parameters: $g_{\parallel} = 2.30$, $A_{\parallel} = 184$ G, $g_{\perp} = 2.04$, $A_{\perp} = 25$ G are calculated from the spectra 1, 2 in Fig. 4. They characterize Cu_{isol}²⁺ ions located in plane square configuration. In spectrum 1 (the preoxidized sample) parameters: $g_{\parallel} = 2, 34$, $A_{\parallel} = 167$ G are also present. It implies that a part of Cu_{isol}²⁺ ions remains in the square pyramidal configuration. We assume that these changes of the spectra are due to the interaction of Cu_{isol}²⁺ ions located both in square pyramidal and plane square configurations with NO₂ molecules (NO₂ molecules are always present in the NO + O₂ mixture). This

interaction seems to result in the formation of a complex which in the following will be referred to as $\text{Cu}^{2+}\text{-O-N=O}$.

TPD spectra of the samples (Cu-containing catalysts and the zeolite free of copper) obtained after the adsorption of the $\text{NO} + \text{O}_2$ mixture at $P=0.8$ kPa, $T=293$ K, and $t=50$ min are presented in Fig. 3. Two peaks were observed on the zeolite free of copper: one (more intensive)—with $T_{\text{max}}=370$ K, and another (more broad)—with $T_{\text{max}}=480$ K (curve 3). In addition to them, the peak with $T_{\text{max}}=620$ K was recorded on the Cu-containing zeolite. For the prereduced sample this peak is larger than for the preoxidized one (see curves 1, 2). The number of molecules (these are mostly NO_2) per 1 g of the catalyst corresponding to this peak is $(7\text{--}4) \times 10^{19} \text{ g}^{-1}$, and this value corresponds closely to the concentration of $\text{Cu}_{\text{isol}}^{2+}$ ions in the oxidized sample ($6 \times 10^{19} \text{ g}^{-1}$). Note that an increase or decrease of copper content in the zeolite leads to a similar change of the peak intensity only at 620 K. A wide peak appeared at 480 K when O_2 gas was adsorbed subsequent to NO adsorption. This peak is present in the TPD spectrum after adsorption of $\text{NO} + \text{O}_2$ mixture (see curves 3, 5).

Thus, after $\text{NO} + \text{O}_2$ adsorption on Cu-containing zeolite, the peaks at 370 and 480 K are due to NO_x desorption from the zeolite matrix and the peak at 620 K is due to NO_2 desorption from $\text{Cu}_{\text{isol}}^{2+}$ ions.

According to ESR data, obtained during the process of thermodesorption, $\text{Cu}^{2+}\text{-O-N=O}$ complexes decay with maximal rate at 600 K (Fig. 6). When the temperature for heating the sample increases, the spectrum is formed which is typical for an oxidized sample before $\text{NO} + \text{O}_2$ adsorption (the lines due to $\text{Cu}_{\text{isol}}^{2+}$ ions in both square pyramidal and plane square configurations appear (Fig. 6, curves 3 and 4).

4. C_3H_8 Adsorption

TPD spectra obtained after C_3H_8 adsorption at room temperature on the reduced and oxidized samples reveal one peak of C_3H_8 desorption with $T_{\text{max}}=370$ K. A similar peak is observed after C_3H_8 adsorption on the zeolite free of copper. The TPD spectrum of C_3H_8 obtained after adsorption of the reaction mixture is similar to that obtained after adsorption of pure C_3H_8 .

We failed to detect any absorption bands in the IR-spectra after C_3H_8 adsorption. The transmittance and diffuse-reflectance techniques were used. Measurements of the intensity of the $\text{Cu}_{\text{isol}}^{2+}$ ESR signal upon treatment of the oxidized samples by pulses of C_3H_8 (1.3 Pa, 5 min) at different temperatures showed that the interaction of C_3H_8 with $\text{Cu}_{\text{isol}}^{2+}$ ions commences after heating the sample above 673 K. This interaction results in the reduction of $\text{Cu}_{\text{isol}}^{2+}$ ions similar to the reduction with hydrogen. The interaction of the copper ions with cracking products appears to be the reason for the reduction, since the reduction temperature coincides with the temperature of propane cracking on zeolite acid sites.

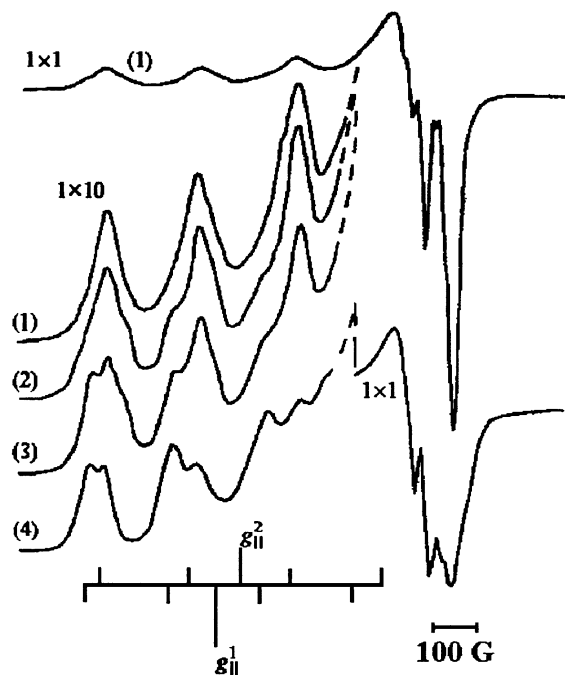


FIG. 6. ESR spectra registered ($P=10^{-4}$ Pa, $T=293$ K) during TPD investigation at 293 K (1), 453 K (2), 573 K (3), 643 K (4).

III. Reactivity of Surface Complexes

Results of the experimental study of the nitrite complex reactivity are shown in Fig. 7. Data are given for 2.8% $\text{CuZ}(1)$ sample. Experiments were carried out in the following way: at 570 K the flow of the $\text{NO} + \text{O}_2$ mixture was replaced by the flow of the $\text{C}_3\text{H}_8 + \text{O}_2$ mixture and the optical density of the absorption band at 1630 cm^{-1} (D) followed (Fig. 7, curve 1). Curve 2 (Fig. 7) represents the results of the first-order equation treatment of curve 1. The runs were conducted at various temperatures (420–570 K) and various concentrations of propane (0.1–1.0%). These data allow one to determine the rate constant for conversion

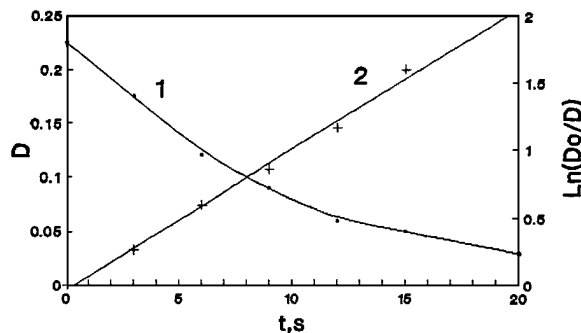


FIG. 7. Time dependence of optical density of the absorption band at 1630 cm^{-1} — D after replacing the $\text{NO} + \text{O}_2$ flow by $\text{C}_3\text{H}_8 + \text{O}_2$ flow at 573 K (1), as well as (2), the result of its treatment in coordinates of the first-order equation, 2.8% $\text{CuZ}(1)$.

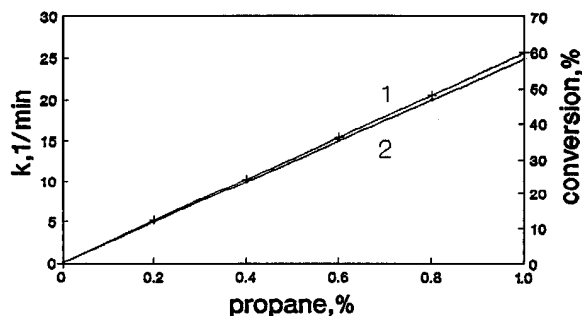


FIG. 8. Dependences of the rate constant of the nitrite complex conversion- k (1) and the NO conversion (2) versus the propane concentration in the reaction mixture, 2.8% Cu₂(1); $T = 573$ K.

of the surface complex assigned to the absorption band at 1630 cm^{-1} . This value and the reaction rate versus the propane concentration are given in Fig. 8.

DISCUSSION

I. Catalytic Activity and State of Copper in the Samples

Let us discuss first the relationship between an exchange level of the sample and its activity in the NO reduction by hydrocarbons. The exchange level of the samples studied in the present work was varied from 5% to 120%. The catalytic activity as shown in Table 2, increases with the exchange level, but not linearly. As the exchange level comes closer to 100%, the growth of the catalytic activity slows down.

These results are in agreement with some published data (62–65). Specifically, Gopalakrishnan *et al.* (62) have reviewed the data for the relationship between an exchange level of the samples and its catalytic activity in the reduction of NO by propane and propene published up to 1992. As was shown there, a 90 to 150% increase of the exchange level does not cause any increase of the catalytic activity. It was shown also for this reaction (Kharas (63)), that the catalytic activity increases with the exchange level, as it increases from 50% to 100%, but it does not change with its further increase up to 450%. The same data, but for NO decomposition, were reported by Iwamoto (2). The catalytic activity increases as the exchange level increases from 40% to 90%, and then stops changing. In (64) evidence is given that the turnover number for SCR of NO increases with the copper dispersion.

All these data allow us to assume that Cu species formed in Cu-ZSM5 materials with a rather low (less than 100%) loading of Cu are the species responsible for the catalytic activity.

Our data demonstrate the coexistence of copper ions (Cu^+ , $\text{Cu}_{\text{isol}}^{2+}$) and aggregates in the samples. The ratio of these species is governed by the pretreatment of the sample and the properties of the zeolite matrix. The $\text{Cu}_{\text{isol}}^{2+}$ ions are

located in two configurations: square pyramidal and plane square. Copper ions (Cu^{2+} , Cu^+) may exist in isolated states inside the zeolite channels, CuO- and Cu_2O -like aggregates (Cu_2) are located on the outer surface of the zeolite.

As was mentioned above (see “Results”), in our samples the $\text{Cu}_{\text{isol}}^{2+}$ ions are very stable and do not undergo auto-reduction. This fact is in contradiction to some published data. The problem of autoreduction of $\text{Cu}_{\text{isol}}^{2+}$ ions in ZSM-5 zeolite has been studied most closely by Larsen *et al.* (65), where it was shown that only a part of $\text{Cu}_{\text{isol}}^{2+}$ ions in the ZSM-5 zeolite undergo autoreduction.

In general, the fact that copper remains in the $\text{Cu}_{\text{isol}}^{2+}$ state after pretreatment is difficult to explain. It is unclear why only part of the copper exchanged into ZSM-5 catalyst as $[\text{Cu}^{2+}\text{OH}^-]^+$ is autoreduced. This might be due to different nature of the sites occupied by $[\text{Cu}^{2+}\text{OH}^-]^+$ (65). If the $[\text{Cu}^{2+}\text{OH}^-]^+$ structures are located near isolated $[\text{AlO}^-\text{Si}]$ charge exchange centers, they would be expected to undergo autoreduction. On other hand, if $[\text{Cu}^{2+}\text{OH}^-]^+$ compensate $[\text{AlO}^-\text{SiO}^-\text{Al}]$ charge exchange centers, the dehydration could be without reduction of Cu^{2+} . This is likely to take place in zeolites with low $\text{SiO}_2/\text{Al}_2\text{O}_3$ ratio and is improbable for high Si zeolites.

Another explanation is given in (66). Starting samples were mentioned (65) to be prepared via Cu acetate and do not contain $[\text{Cu}-\text{OH}]^+$, but have $[\text{Cu}-\text{OCOCH}_3]^+$ species strongly bonded at the cationic position. Therefore, subsequent treatment of these samples either in a vacuum or in a He flow may be accompanied by partial reduction of cupric ions by organic species retained in the zeolite. We suppose that the explanation given in (66) is more realistic.

As is seen from Fig. 2, concentration of $\text{Cu}_{\text{isol}}^{2+}$ ions and the activity of the sample in the reduction of NO with propane are correlated. Concentration of $\text{Cu}_{\text{isol}}^{2+}$ ions can be lowered both by diminishing the level of exchange when preparing the sample and by using NaZSM-5 zeolite. In the latter case, the rate of exchange procedure is lower than that of exchanging H^+ with Cu ions. In our work, the exchange of both H- and Na zeolite forms was carried out during the same time (6 h). As a result, part of the sites in the NaZSM-5 zeolite, which could be occupied by Cu, was blocked by Na and, hence, the concentration of $\text{Cu}_{\text{isol}}^{2+}$ ions drops. The activity of the sample decreases with the decreasing concentration of $\text{Cu}_{\text{isol}}^{2+}$ ions in both cases.

It is impossible to specify which $\text{Cu}_{\text{isol}}^{2+}$ ions (in terms of configuration) are responsible for the reaction, since the ratio of numbers of ions in various configurations is virtually constant for all the samples studied. However, it is known (52, 53) that the most coordinatively unsaturated $\text{Cu}_{\text{isol}}^{2+}$ ions have the greatest catalytic activity. In the case of Cu-containing ZSM-5 zeolites, these are the $\text{Cu}_{\text{isol}}^{2+}$ ions in the plane square configuration.

The correlation shown in Fig. 2 points to the fact that the limiting stage of the process proceeds on the $\text{Cu}_{\text{isol}}^{2+}$ ions.

Data obtained by ESR, TPD, and IR spectroscopy allow us to discuss the nature of the intermediate in this stage.

It was found that:

(1) Some weak complexes of Cu^{2+} are formed on the surface when NO and O_2 are adsorbing at room temperature, which decay at pumping out the gas. No surface complexes combined C_3H_8 and Cu ions were detected.

(2) At the reaction temperature (600–900 K) the interaction of the sample with oxygen or propane causes the oxidation ($\text{Cu}^+ \rightarrow \text{Cu}^{2+}$) or the reduction ($\text{Cu}^{2+} \rightarrow \text{Cu}^+$) of copper, respectively. When NO interacts with the sample, the state of the copper does not change at all.

(3) TPD data show that NO and O_2 are adsorbed mostly on the zeolite itself, and the number of adsorbed NO molecules is essentially higher than the number of oxygen molecules, NO high-temperature TPD peaks of NO were recorded, contrary to some published data (64). This is likely because of the difference of the samples studied (pretreatment and so on). Indeed, the high-temperature peak is usually observed in the TPD-spectra after the adsorption of NO on the oxidized sample and is not observed under the same conditions on the reduced ones (55, 67).

(4) The most interesting results were obtained for the adsorption of the NO + O_2 mixture:

IR-spectroscopy. An absorption band at 1630 cm^{-1} appears in the IR-spectra *in situ* (the same absorption band is observed in the IR-spectra under the reaction conditions). It is not due to the adsorption of water, since it appears only after adsorption of the NO + O_2 mixture (and it does not appear after the adsorption of NO). Besides, this band is observed in the spectra at rather high temperatures when there are no absorption bands of water in the IR-spectra at all.

ESR and TPD. At the adsorption of the NO + O_2 mixture a new, rather thermostable complex is formed. At above 620 K this complex decomposes with an activation energy of 145 kJ/mol. It is, possibly, due to the entering of NO_2 molecules into ligands of the $\text{Cu}^{2+}_{\text{isol}}$ ion. The number of desorbed NO_2 molecules in the 480–700 K range is rather close to the number of $\text{Cu}^{2+}_{\text{isol}}$ ions, so, on average, near every $\text{Cu}^{2+}_{\text{isol}}$ ion there is at least one NO_2 ligand. Consequently, the square planar configuration of this complex is likely to be formed from the NO_2 molecule and three oxygen atoms from the zeolite. We do not discuss here in detail the electronic structure of this complex.

Thus, it is possible to say that here, by a variety of methods, we observe one and the same surface complex. According to (10), the $\text{Cu}^{2+}\text{-O-N=O}$ structure was assigned to it.

Spectrokinetic data show that the relationship between the concentration of this (nitrite) complex and the oxygen content in the mixture is similar to the relationship between the rate of NO_x neutralization and this parameter (Fig. 9).

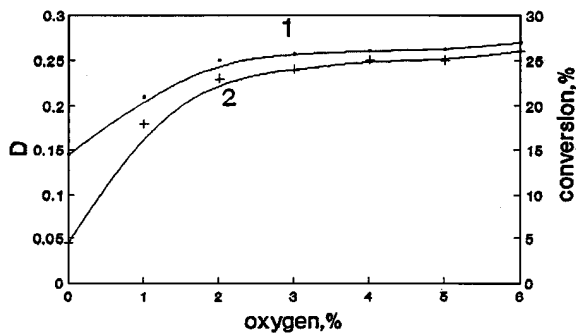


FIG. 9. Dependences of the nitrite complex concentration— D (1) and the NO conversion (2) versus the oxygen content in the reaction mixture, 2.8% CuZ(1); $T = 573\text{ K}$.

On other hand, the relationship between the rate constant of the nitrite complex conversion and the propane concentration in the mixture is similar to the relationship between the rate of NO_x neutralization and this parameter (Fig. 8).

These facts are evidence in favor of an assumption that transformation of this complex is the rate-determining step of the process.

II. Reactivity of Surface Nitrite Complexes

To prove the above-mentioned assumption, we correlate the rate of the nitrite complex conversion with the reaction rate. As is seen from Fig. 10, the optical density of the absorption band of the nitrite complex (D) at 573 K is 0.05. It means that there are $N = DS/\varepsilon = 3 \times 10^{16}$ complexes in the sample (here, D is an optical density of the absorption band, S is the surface of the sample, and ε is the extinction coefficient. The procedure of ε determining is described in (68)). If NO_x reduction proceeds via this complex, the reaction rate is $W = k * N = 1.8 * 10^{17}$ molecule/min. (The value of k obtained from the results shown in Fig. 7 is 6 min^{-1}). The experimental value of the reaction rate for this sample is $W = 2.2 * 10^{17}$ molecule/min. The coincidence of these two values (the rate of the complex conversion and the reaction

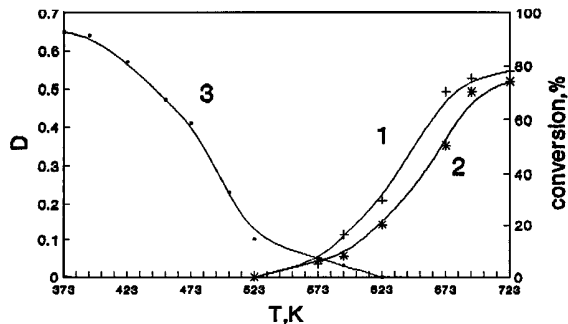


FIG. 10. Temperature dependencies of (1) C_3H_8 and (2) NO conversion; (3) optical density of the absorption band at 1630 cm^{-1} (D), 2.8% CuZ(1).

rate) proves that the nitrite complex is an intermediate in the reduction of NO with propane. Thus, in this reaction, NO activation is connected with the formation of the surface nitrite complex on Cu_{isol}²⁺ ions. This conclusion allows us to explain easily the fact that the efficiency of the reduction of NO₂ is higher than that of NO (see, for example, (3)).

From the temperature dependence of the rate constant the activation energy (80 kJ/mol) was determined. Linear dependence of the rate constant on propane concentration points to the first-order consumption of the surface complex on propane (Fig. 8).

However, the further conversion of the nitrite complex is not clear yet. It interacts possibly with adsorbed hydrocarbon molecules or hydrocarbon fragments. Hydrocarbon fragments, formed after the interaction of C_nH_m molecules with the acid sites of the zeolite, could possibly play an important role in the reaction. More investigations are necessary to answer this question.

So, the Cu²⁺-O-N=O complex is proved to be an intermediate in the reduction of NO by propane with excess oxygen. It implies, possibly, that Cu_{isol}²⁺ ions are active sites of the catalyst. This point of view is consistent with the published data (see "Introduction"), where Cu_{isol}²⁺ ions, among other states of exchanged copper in the samples, are considered as active sites of the catalyst. Also conversions between Cu(I) and Cu(II) are reported to be important for the reaction, as well as conversions between ions and clusters of copper.

And yet, we think that contradictions between the different points of view on the nature of an active site of the catalyst are more apparent than real. Indeed, the selective catalytic reduction of NO is a complex multistage process, involving adsorption of reagents, formation of intermediate complexes, and so on. Different stages of the reaction may, possibly, proceed on different surface sites. So, NO molecules may need Cu_{isol}²⁺ ions for adsorption with following the formation of the Cu²⁺-O-N=O complex, while hydrocarbons may adsorb on both Cu⁺ ions (11) and copper aggregates. Also some other states of copper (possibly, pairs of sites) may serve as centers where the intermediate complexes are formed. It seems likely that various investigators observe various stages of the reaction, and, therefore, form various concepts of its active site. From this point of view, we have observed one of the first stages of the reaction—the activation of NO and the Cu_{isol}²⁺ ion needed for this stage to proceed, is part of a complex active site of the whole reaction.

III. The Role of Oxygen in the Reaction

The role of oxygen in the reaction has been discussed in some detail in the review by Shelef (69). Our data confirm his point of view on the problem, at least on two counts:

First, according to ESR data, under reaction conditions the catalyst is oxidized. Its activity correlates well with an

amount of bivalent copper ions in the sample. So, oxygen is likely to keep copper ions in an oxidized state (13).

Second, as was mentioned above, oxygen in the reaction mixture promotes the NO activation by producing the surface nitrite complexes.

However, we do not know yet, why, in the presence of a great excess of oxygen, hydrocarbons interact mainly with NO, instead of the oxygen. The situation is, possibly, that both molecular and dissociative adsorption of oxygen over Cu-containing zeolites are hindered. Oxygen molecules cannot be bound strongly with oxidized copper ions. And dissociative adsorption is very unlikely, too, since for it close-placed Cu sites are needed. In other words, oxygen adsorption on isolated Cu²⁺ ions is hindered, whereas NO forms nitrite complexes rather easily. Evidently, just this property of the system makes possible the reduction of NO in the presence of oxygen.

CONCLUSIONS

Our data demonstrate the coexistence of various states of copper (Cu⁺, Cu_{isol}²⁺, and CuO-, Cu₂O-like aggregates) in the sample, even at relatively low amounts of exchanged copper. The ratio of these species is governed both by pretreatment of the sample and properties of the zeolite matrix. The Cu_{isol}²⁺ ions are characterized by two configurations: square pyramidal and plane square. Copper ions (Cu²⁺, Cu⁺) may exist in isolated states inside the zeolite channels, CuO-, Cu₂O-like aggregates (Cu_a) are located on outer surface of the zeolite.

Activity of the samples in the reduction of NO by propane correlates rather well with concentration of Cu_{isol}²⁺ ions.

On the basis of ESR, TPD, and IR-spectroscopy *in situ* data, the Cu²⁺-O-N=O complex is found to be formed on the surface of Cu-containing zeolites under the reaction conditions. The rate of its following transformation to the reaction products was measured by the spectrokinetic method and appeared to be equal to the reaction rate. Coincidence of these two values implies that the Cu²⁺-O-N=O complex is a true intermediate in this reaction and takes part in the rate-determining stage.

Cu_{isol}²⁺ ions in the samples studied are the centers where one of the first stages of the reaction (NO activation) proceeds. Next stages occur, possibly, over other surface states of the copper. From this point of view, the Cu_{isol}²⁺ ion is a necessary part of the complex active center of the reaction. The mechanism of its further transformation is not clear yet, and some more experiments are needed to clarify it.

REFERENCES

1. Iwamoto, M., Yahiro, H., and Tanda, K., *J. Phys. Chem.* **95**, 3727 (1991).
2. Iwamoto, M., Yahiro, H., Mizuno, N., Xhang, W.-X., Mine, Y., Furukawa, H., and Kagawa, S., *J. Phys. Chem.* **96**, 9360 (1992).

3. Iwamoto, M., in "Proc., Meeting of Catalytic Technology for Removal of NO, Tokyo, 1990," p. 17.
4. Valyon, J., and Hall, W. K., *J. Phys. Chem.* **97**, 5211 (1993).
5. Shpiro, E. S., Grunert, W., Joyner, R. W., and Baeva, J. N., *Catal. Lett.* **24**, 159 (1994).
6. Sarkani, J., d'Itri, J. L., and Sachtler, W. M. H., *Catal. Lett.* **16**, 242 (1992).
7. Shelef, M., *Catal. Lett.* **15**, 305 (1992).
8. Iwamoto, M., Yahiro, H., Mizuno, K., Zhang, W. X., Miye, Y., and Furukawa, H., *J. Phys. Chem.* **96**, 9360 (1992).
9. Ansell, G. P., Diwail, A. F., and Golunski, S. E., *Appl. Catal. B* **2**, 81 (1993).
10. Larsen, S., Aylor, A. W., Bell, A. W., and Reimer, J. A., in "Proc. U.S.-Russia Workshop on Environmental Catalysis, Wilmington, Delaware, 1994," p. 21.
11. Hayes, N., Joyner, R. W., and Shapiro, E. S., *Appl. Catal. B* **8**(3), 341 (1996).
12. Hayes, N. W., Grunert, W., Hutchings, G. J., Joyner, R. W., and Shapiro, E. S., *J. Chem. Soc. Chem. Commun.* **531** (1994).
13. Burch, R., and Millingham, P., *J. Appl. Catal. B* **2**, 71 (1993).
14. Yahiro, H., Yu-u, Y., Takeda, H., Mizuno, H., and Iwamoto, M., *Shokubai.* **15**, 130 (1993).
15. Sasaki, M., Hamada, H., Kintaichi, H., and Ito, T., *Catal. Lett.* **15**, 297 (1993).
16. Petunchi, J. O., Sill, G., and Hall, W. K., *Appl. Catal. B* **2**, 303 (1993).
17. Yasuda, H., Miyamoto, T., Yokoyama, C., and Misono, M., *Shokubai.* **35**, 386 (1993).
18. Yokoyama, C., Yasuda, H., and Misono, M., *Shokubai.* **35**, 122 (1993).
19. Tabata, T., and Kokitsu, M., *Catal. Lett.* **25**, 393 (1994).
20. Yogo, K., Ihara, M., Terasaki, I., and Kikuchi, E., *Chem. Lett.* **2**, 229 (1993).
21. Yogo, K., Ihara, M., Terasaki, I., Watanabe, H., and Kikuchi, E., *Shokubai.* **35**, 126 (1993).
22. Naito, S., and Tanimoto, M., *Chem. Lett.* **11**, 1935 (1993).
23. Sadykov, V. A., Rozovskii, A. Ya, Lunin, V. V., and Matyshak, V. A., in "Proc. U.S.-Russia Workshop on Environmental Catalysis, Wilmington, Delaware, 1994," p. 20.
24. Centi, G., Perattone, S., Biglino, D., and Giamello, E., *J. Catal.* **151**, 75 (1995).
25. Koutyrev, M. Yu., Ukharchkii, A. A., Il'ichev, A. N., and Matyshak, V. A., in "Proc. First World Conference Environmental Catalysis, Pisa, Italy, 1995," p. 311.
26. Sadykov, V. A., Alikina, G. M., and Bunina, R. V., in "Proc. First World Conference Environmental Catalysis, Pisa, Italy, 1995," p. 315.
27. Valyon, J., and Hall, W. K., *J. Phys. Chem.* **97**, 1205 (1993).
28. Zhang, B., Yamaguchi, T., Kawakami, H., and Suzuki, T., *Appl. Catal. B* **1**, L15 (1992).
29. Petunchi, J. O., and Hall, W. K., *Appl. Catal. B* **2**, L17 (1993).
30. Hamada, H., Kintaichi, Y., Sasaki, M., and Ito, T., *Appl. Catal.* **70**, L15 (1991).
31. Hamada, H., Kintaichi, Y., Sasaki, M., Ito, T., and Tabata, M., *Appl. Catal.* **75**, L1 (1991).
32. Yokoyama, Ch., and Misono, M., *J. Catal.* **150**, 9 (1994).
33. Sadykov, V. A., Baron, S. L., Matyshak, V. A., Alikina, G. M., Bunina, R. V., Rozovskii, A. Ya., Lunin, V. V., Lunina, E. V., Kharlanov, A. N., Ivanova, A. S., and Veniaminov, A. S., *Catal. Lett.* **37**, 157 (1996).
34. Bennett, C. J., Bennett, P. S., Golunski, S. E., Hages, J. W., and Walker, A. P., *Appl. Catal.* **86**, L1 (1992).
35. Teraoka, Y., Ogawa, H., Furukawa, H., and Kagawa, S., *Catal. Lett.* **12**, 261 (1992).
36. Iwamoto, M., Yashiro, H., Ooe, H., Banno, K. Y., and Okamoto, F., *Shokubai.* **32**, 91 (1990).
37. Torikai, Y., Yahiro, H., Mizuno, N., and Iwamoto, M., *Catal. Lett.* **9**, 91 (1991).
38. Burch, R., and Millingham, P. J., *Appl. Catal. B* **2**, 101 (1993).
39. Inui, T., Kojo, S., Shibata, M., Yoshida, T., and Iwamoto, M., *Stud. Surf. Sci. Catal.* **69**, 355 (1991).
40. Iwamoto, M., presented at the "ACS Meeting, 1993," paper 23.
41. Cho, B. K., *J. Catal.* **155**(2), 184 (1995).
42. Ansell, G. P., Diwail, A. F., Golunski, S. E., Hayes, J. M., Rayaram, R. R., and Walker, A. P., *Appl. Catal. B* **1**, 1 (1992).
43. Kucherov, A., Gerlock, J. L., Jen, H-W., and Shelef, M., *J. Catal.* **152**, 63 (1995).
44. Grunert, W., Hayes, N. W., Joyner, R. W., Spiro, E. S., Siddiqui, M/R. H., and Baeva, G. N., *J. Phys. Chem.* **98**, 10832 (1994).
45. Marques-Alvarez, C. M., Rodrigues-Ramos, I., Fernandes-Garcia, M., and Haller, G. L., in "Proc. 11th Int. Congr. on Catal., 1996," p. 206.
46. Yan, J. Y., Lei, G. D., Sachtler, W. M. H., and Kung, H. H., in "Proc. 11th Int. Congr. on Catal.," p. 211.
47. Iwamoto, M., *Stud. Surf. Sci. Catal.* **54**, 121 (1990).
48. Iwamoto, M., Yahiro, H., Shundo, S., Yu-u, Y., and Mizuno, M., *Appl. Catal.* **69**, L15 (1991).
49. Li, L., and Hall, W. K., *J. Catal.* **129**, 202 (1991).
50. Ebitani, K., Morokuma, M., and Morikawa, N., Zeolites and related microporous materials. State of the art, *Stud. Surf. Sci. Catal.* **84**, 1501 (1994).
51. Iwamoto, M., *Stud. Surf. Sci. Catal.* **84**, 1395 (1994).
52. Sass, C. E., and Kevan, L., *J. Phys. Chem.* **93**, 7856 (1989).
53. Kucherov, A. V., Kucherova, T. H., and Slinkin, A. A., *Kinet. Katal.* **33**, 706 (1992).
54. Kucherov, A. V., and Slinkin, A. A., *Usp. Khim.* **61**, 1687 (1992).
55. Il'ichev, A. N., Ukharchkii, A. A., and Matyshak, V. A., *Kinet. Katal.* **36**, 268 (1995).
56. Kucherov, A. V., and Slinkin, A. A., *Kinet. Katal.* **27**, 585 (1986).
57. Davydov, A. A., IK-Spektroskopiy v khimii Poverkhnosti Oksidov (IR-spectroscopy applied to the chemistry of oxide surface), Novosibirsk, 1984.
58. Matyshak, V. A., *Kinet. Katal.* **30**(1), 38 (1989).
59. Matyshak, V. A., and Krylov, O. V., *Catal. Today* **25**(1), 1 (1995).
60. Kucherov, A. V., Slinkin, A. A., Kondrat'ev, D. V., Bondorenko, T. N., Rubinshtein, A. M., and Minachev, H. M., *Kinet. Katal.* **26**, 353 (1985).
61. Anpo, M., Nomyra, T., and Shioya, Y., in "Proc. 10th Int. Congress on Catalysis, Budapest, 1993," p. 2154.
62. Gopalakrishnan, R., Stafford, P. R., Davidson, J. E., Hecker, C. W., and Bartholomew, C. H., *Appl. Catal. B* **2**, 165 (1993).
63. Kharas, K. C. C., *Appl. Catal. B* **2**, 207 (1993).
64. Shapiro, E. S., Joyner, W. R., Grunert, W., Hayes, N. W., Siddiqui, M. R. H., and Baeva, G. N., *Stud. Surf. Sci. Catal.* **84**, 1483 (1994).
65. Larsen, S. C., Aylor, A., Bell, A. T., and Reimer, J. A., *J. Phys. Chem.* **98**(44), 11533 (1994).
66. Kucherov, F. V., Slovetskaya, K. I., Goryaschenko, S. S., Aleshin, E. G., and Slinkin, A. A., *Microporous Mat.* **7**, 27 (1996).
67. Li, Y., and Armor, J. N., *Appl. Catal.* **76**(2), L1 (1991).
68. Matyshak, V. A., Baron, S. L., Il'ichev, A. N., Ukharchkii, A. A., Sadykov, V. A., and Korchak, V. N., *Kinet. Katal.* **37**, 585 (1996).
69. Shelef, M., *Chem. Rev.* **95**, 209 (1995).